Theory of excitons in the insulating Cu-O_2 plane

F. C. Zhang
Department of Physics, University of Cincinnati, Cincinnati, Ohio 45221

K. K. Ng
Department of Physics, University of Cincinnati, Cincinnati, Ohio 45221
and Yukawa Institute for Theoretical Physics, Kyoto University, Kyoto 606-8502, Japan
(Received 6 April 1998)

We use a local model to study the formation and the structure of the low-energy charge-transfer excitations in the insulating Cu-O_2 plane. The elementary excitation is a bound exciton of spin singlet, consisting of a Cu^+ and a neighboring spin singlet of Cu-O holes. The exciton can move through the lattice freely without disturbing the antiferromagnetic spin background, in contrast to the single hole motion. There are four eigenmodes of excitons with different symmetry. The p-wave-like exciton has a large dispersion width. The s-wave-like exciton mixes with the p state at finite momentum, and its dipole transition intensity is strongly anisotropic. The model is in excellent agreement with the electron energy-loss spectra in the insulating $Sr_2CuO_2Cl_2$. [S0163-1829(98)04144-7]

I. INTRODUCTION

There have been extensive efforts in recent years on the electronic structure in the layered Cu oxides, in the hope to reveal the mechanism for the high T_c superconductivity. It is now well established that the low-energy physics of the undoped cuprates is well described by the spin-1/2 Heisenberg model in a square lattice, leading to an antiferromagnetic insulator. A two-dimensional t-J model has been proposed and argued to describe the low-energy physics for the cuprates,[1,2] and it seems the model explains many unusual properties of the high-T_c materials.

In this paper we present a theory for the lower energy charge-transfer excitations in the insulating Cu-oxide plane. Our work was motivated by the angle-resolved electron-energy-loss spectra (EELS) in the insulating $Sr_2CuO_2Cl_2$, where the optical allowed transition shows a large energy dispersion width of 1.5 eV, and the optical forbidden transition was observed to be strongly anisotropic.[3]

We use a local model to analyze the formation and the structure of the charge transfer excitation between Cu $3d_{x^2-y^2}$ and O $2p\sigma$ in the Cu-oxide planes. The elementary charge-transfer excitation is a bound exciton of spin singlet, consisting of a Cu^+ (quasiparticle) and a neighboring spin singlet of Cu-O holes. The exciton can move through the lattice freely without disturbing the antiferromagnetic (AF) spin background, in contrast to the single-hole motion. There are four exciton modes related to the fourfold rotation symmetry in the lattice, whose hopping matrices determine the dynamics and the symmetry of the charge-transfer excitations. The p-wave-like exciton has a large energy dispersion width. The s-wave-like exciton mixes with the p state at finite $\mathbf{k}$, and its optical transition intensity is strongly anisotropic. The model is in excellent agreement with the recent electron energy-loss spectra in the insulating $Sr_2CuO_2Cl_2$. The theory also predicts a lower energy optical forbidden mode, which should be observable in the luminescence experiment.[4] Since the mass of the particle-hole pair is heavier than the particle or the hole in a usual semiconductor or in other bandlike insulator materials,[5] the anomalous behavior of the dispersion widths between the single hole and the exciton in cuprates provides further evidence for the strong correlation in these compounds. A part of the results in this paper was briefly reported in a paper with the EELS experiments.[3] The paper is organized as follows. In Sec. II, we examine the formation and the structure of small excitons in the insulating cuprates. The dynamics of the excitons is derived in Sec. III. The exciton eigenmodes and the relevance to the charge-transfer gap and to the EELS are described in Sec. IV. Several remarks and discussions are made in Sec. V.

II. STRUCTURE OF SMALL EXCITONS

We consider a Cu-oxide plane, where the vacuum is the filled shell states of Cu^+ and O^{2-}. In the undoped case, there is one hole in average in each unit cell of CuO_2, and the hole primarily resides on the Cu site and is of $d_{x^2-y^2}$ symmetry. Because of the strong on-site Coulomb repulsion between the Cu holes, the ground state is a spin-1/2 antiferromagnet of Cu^{2+}. To study the low-energy charge excitations of a particle-hole pair, we shall focus on the transition from the Cu $3d_{x^2-y^2}$ to O $2p\sigma$ states. This transition is of particular interest due to the relatively small atomic energy difference and due to the large orbital overlap between the two states, hence the strong intensity in experiments. The measured optical gap[6] is related to this transition.

Let us start with a local pair of particle and hole and examine the formation and the structure of the exciton. As illustrated in Fig. 1, the quasiparticle is at a vacant Cu site (Cu^+), and the quasihole is at the O site. There are two important physical effects for the pair. The first is the Coulomb attraction between the particle and the hole, which should be considerably large in the insulating compounds where the screening effect is weak. It is this attraction to bind the pair to form an exciton. For simplicity we shall assume

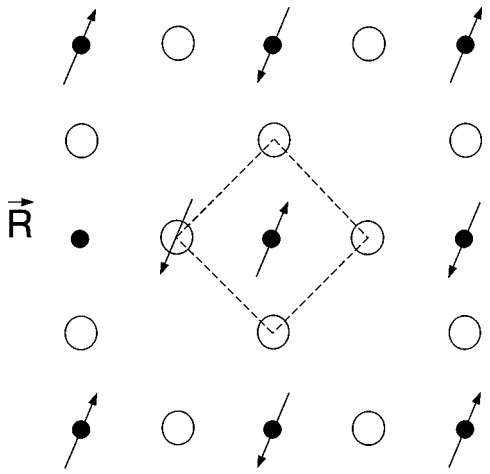

FIG. 1. The structure of a local exciton in the CuO_2 plane. The open circles represent O atoms, solid circles represent Cu atoms, the arrows represent spins of holes. The quasiparticle (Cu^+) is at the vacant Cu site R, and the quasihole is on the square of O atoms and forms a spin singlet with the central Cu hole.

the attractive potential to be short-ranged, which is $-E_c<0$ when the particle and hole are nearest neighbors (NN), and is zero otherwise. We expect that the more realistic potentials will not change the basic physics as long as the NN attraction dominates. The second is the strong Cu-O hybridization which binds a hole on each square of O atoms to the central Cu hole to form a spin singlet.[2] Let us denote this binding energy to be E_s. As a compromise of the above two effects, we expect a spin singlet with more weight of the O hole on the site near the Cu^+. We can make the above argument more quantitatively using a variation approach. Let the O-hole state be

$$\Phi=\alpha P_{-\hat{x}/2}+\beta(-P_{\hat{x}/2}+P_{\hat{y}/2}-P_{-\hat{y}/2}), \tag{1}$$

where P is the atomic O-hole orbital, whose subindex denotes the atomic position relative to their central Cu hole (lattice constant 1), and $P_{-\hat{x}/2}$ is the one close to the Cu^+. The total binding energy of the exciton E_b takes maximum when $\alpha^2=(1+1/\sqrt{1+3c})/2$, with $c=E_s^2/(2E_c-E_s)^2$. Typically, $\alpha^2=0.5$ or 0.75 for $E_c/E_s=0.5$ or 1. From the above analysis we see that the exciton in cuprates is a complex object, consisting of a Cu^+ and a nearby Cu-O singlet. The spin-triplet exciton energy has a binding energy of E_c, smaller than the binding energy E_b of the spin-singlet exciton, and will not be considered in this paper.

The parameters E_c and E_s in cuprates should be within certain regions so that the system is stable against the excitonic excitations. Let ϵ_p be the atomic energy difference between the Cu- and O-hole states, the stability condition in the local limit is $E_b<\epsilon_p$. If we further consider an extra hole (primarily residing on O-site) in the half-filled insulating Cu oxides, the model system should be stable against excitonic excitation (one of the Cu holes moves to the oxygen). This implies $2E_b<\epsilon_p+E_s$. Our discussion in this paper will be limited to the above physical parameter region.

There are four spin-singlet exciton states for a fixed quasiparticle at $\mathbf{R}$, denoted by $\tau(\mathbf{R})$, where τ is the coordinator of the Cu site in the singlet relative to $\mathbf{R}$. $\tau=\hat{x}$, $-\hat{x}$, $\hat{y}$, and $-\hat{y}$. These will be briefly denoted by x, $\bar{x}$, y, and $\bar{y}$, respectively.

III. DYNAMICS OF EXCITONS

The exciton can move through the lattice due to the NN Cu-O hopping t_{pd} and the O-O direct hopping t_{pp}. The most important feature of the exciton dynamics is that the exciton motion does not disturb the AF spin background. This is because each exciton involves two neighboring Cu sites, and both are spinless. As far as spins are concerned, the spin-singlet exciton is similar to a pair of bound NN holes, whose motion does not disturb the AF spin background. This property should be compared with the single-hole dynamics in Cu oxide, where the AF spin background is strongly disturbed, and the hole dispersion is given by the Cu-Cu spin exchange interaction J instead of the hole-hopping integral t, as shown theoretically for the t-J model[7] and observed in the recent angle-resolved photoemission experiments.[4]

We now study the exciton motion quantitatively. A general hopping process of the exciton in the coordinator space may be represented by $\tau(\mathbf{R})\rightarrow\tau'(\mathbf{R}')$ with the hopping integral $t_{\tau\tau'}(\mathbf{R}'-\mathbf{R})$. Because the AF spin background is unchanged,[8] the exciton motion is equivalent to that for a free particle. Let $|GS\rangle$ be the AF ground state, and $\gamma_\tau^\dagger(\mathbf{R})$ is an operator to create an exciton $\tau(\mathbf{R})$ in the ground state, so that $\gamma_\tau^\dagger(\mathbf{R})|GS\rangle$ is the state of exciton $\tau(\mathbf{R})$ in an otherwise AF spin background. The exciton hopping is described by an effective Hamiltonian H_{eff}, which acts on the Hilbert space of the single exciton states,

$$H_{eff}\gamma_\tau^\dagger(\mathbf{R})|GS\rangle=\sum_{\mathbf{R}',\tau'} t_{\tau\tau'}(\mathbf{R}-\mathbf{R}')\gamma_{\tau'}^\dagger(\mathbf{R}')|GS\rangle. \tag{2}$$

It follows that

$$H_{eff}=\sum_{\mathbf{k}} \gamma^\dagger(\mathbf{k})T(\mathbf{k})\gamma(\mathbf{k}), \tag{3}$$

with $\gamma^\dagger(\mathbf{k})=(\gamma_x^\dagger,\gamma_{\bar{x}}^\dagger,\gamma_y^\dagger,\gamma_{\bar{y}}^\dagger)$. $T(\mathbf{k})$ is a 4×4 matrix, which determines the exciton dynamics, and $T_{\tau\tau'}(\mathbf{k})=\Sigma_{\mathbf{r}}t_{\tau\tau'}(\mathbf{r})e^{i\mathbf{k}\cdot\mathbf{r}}/N$, with N the number of Cu sites. Note that $\mathbf{k}$ is in the whole first Brillouin zone although there are two sublattices in the ground state. The matrix is hermitian, $T_{\tau\tau'}(\mathbf{k})=T^*_{\tau'\tau}(\mathbf{k})$. Because $t_{\tau\tau'}(\mathbf{r})$ is real, we have $T_{\tau\tau'}(\mathbf{k})=T^*_{\tau\tau'}(-\mathbf{k})$. The Cu-O plane has certain symmetries. Taking into account of the Cu- and O-hole orbital symmetries, we have $T_{\tau\tau'}(\mathbf{k})=T_{\bar{\tau}\bar{\tau}'}(-\mathbf{k})$ from the parity invariance, $T_{x\bar{y}}(k_x,k_y)=-T_{xy}(k_x,-k_y)$ from the inversion symmetry with respect to the x axis, and $T_{x\bar{x}}(k_x,k_y)=T_{y\bar{y}}(-k_y,k_x)$ due to the fourfold rotational invariance.

To pursue the theory further, we estimate the hopping integral $t_{\tau\tau'}(\mathbf{r})$ within the atomic limit and treat t_{pd} and t_{pp} perturbatively. We shall consider the limit $\alpha=1$ in Eq. (1) for simplicity and for the purpose of illustration. Up to the third order in perturbation in t_{pd} or t_{pp}, there are only four nonzero independent integrals:

$$t_1\equiv t_{xy}(0)=\frac{1}{2}(t_{pp}-t_{pd}^2/\epsilon_p),$$

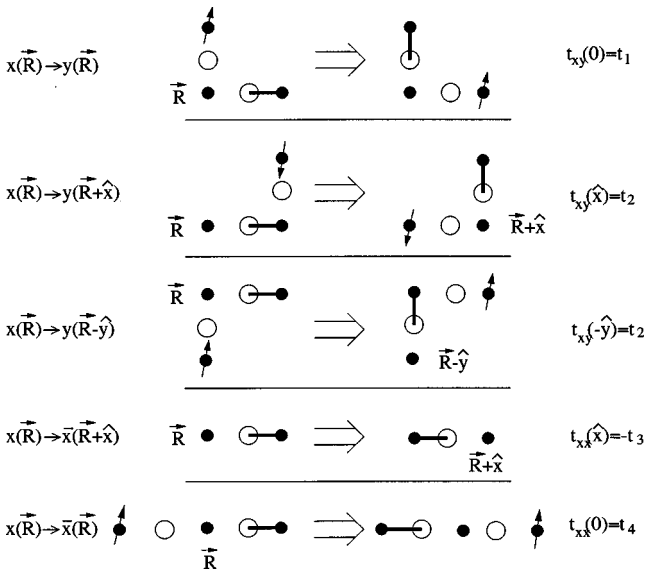

FIG. 2. A list of the five most important hopping processes from $x(\mathbf{R})$ to $\bar{x}(\mathbf{R}')$ and $y(\mathbf{R}')$. The open and solid circles represent the same as in Fig. 1. The thick line between a O and a Cu represents a spin singlet of holes on the two sites. Not shown are the antiferromagnetic background of Cu spins and empty O holes in the lattice. The other hoppings can be obtained by symmetry. The corresponding effective hopping integrals are given by Eq. (4).

$$t_2 \equiv t_{xy}(\hat{x}) = t_{pp} t_{pd}^2/(2\epsilon_p E_c),$$
$$t_3 \equiv -t_{x\bar{x}}(\hat{x}) = t_{pd}^2[\epsilon_p^{-1} - (\epsilon_p + U_{pp})^{-1}], \tag{4}$$
$$t_4 \equiv t_{x\bar{x}}(0) = t_{pd}^2/(2\epsilon_p).$$

A diagrammatic illustration for these hopping processes is shown in Fig. 2. In Eq. (4), U_{pp} is the on-site O-hole Coulomb repulsion. We have kept the third order term t_2 because E_c is small compared to ϵ_p. From Eq. (4), $t_3 > t_4$. Since $t_{pp} > 0$ for the oxygen hole hopping, t_2, t_3, and t_4 are all positive. Using these t's and the symmetries discussed above, we obtain

$$T(\mathbf{k}) = \begin{pmatrix} 0 & a(k_x) & b(\mathbf{k}) & \bar{b}(\mathbf{k}) \\ a^*(k_x) & 0 & \bar{b}^*(\mathbf{k}) & b^*(\mathbf{k}) \\ b^*(\mathbf{k}) & \bar{b}(\mathbf{k}) & 0 & a(k_y) \\ \bar{b}^*(\mathbf{k}) & b(\mathbf{k}) & a^*(k_y) & 0 \end{pmatrix}, \tag{5}$$

where $\bar{b}(k_x, k_y) = -b(k_x, -k_y)$, and

$$a(k_x) = t_4 - t_3 e^{ik_x},$$
$$b(\mathbf{k}) = t_1 + t_2(e^{ik_x} + e^{-ik_y}). \tag{6}$$

IV. EXCITON EIGENMODES

H_{eff} can be diagonalized to obtain the exciton solutions. For $\mathbf{k}$ along the [11] direction, the analytical solutions are particularly simple and are listed in Table I. At $\mathbf{k}=0$, the four exciton eigenstates have well-defined local symmetry,[9] describing the uniformly moving molecular states. They are illustrated in Fig. 3. The s- and d-wave states are given by

TABLE I. Solutions of the four-exciton modes for $\mathbf{k}$ along the [11] direction. The $\mathbf{k}$ dependence in a, b, and $\bar{b}$ is implied, see Eq. (5). $\eta_\pm = \frac{1}{2}(a \pm \bar{b})/|a \pm \bar{b}|$. The last column applies to the region $(-b_0 < a_0 < b_0)$ suitable to cuprates, and a_0, b_0 are their values at $k=0$.

Mode	Energy	Eigenstate	Symmetry at $\mathbf{k}\to 0$
P_1	$-b+\lvert a-\bar{b}\rvert$	$(-\eta_-, -1/2, \eta_-, 1/2)$	p_1
P_2	$b-\lvert a+\bar{b}\rvert$	$(-\eta_+, 1/2, -\eta_+, 1/2)$	p_2
S	$b+\lvert a+\bar{b}\rvert$	$(\eta_+, 1/2, \eta_+, 1/2)$	s
D	$-b-\lvert a-\bar{b}\rvert$	$(\eta_-, -1/2, -\eta_-, 1/2)$	$d_{x^2-y^2}$

$$|s\rangle = \left(-\frac{1}{2}, \frac{1}{2}, -\frac{1}{2}, \frac{1}{2}\right),$$
$$|d\rangle = \left(-\frac{1}{2}, \frac{1}{2}, \frac{1}{2}, -\frac{1}{2}\right), \tag{7}$$

where the four components represent the amplitudes of the excitons $\gamma_x, \gamma_{\bar{x}}, \gamma_y, \gamma_{\bar{y}}$, respectively. The energies for the s and d states are $2b_0 - a_0$, and $-2b_0 - a_0$, respectively, where a_0 and b_0 are their values at $\mathbf{k}=0$, and $a_0 = t_4 - t_3 > 0$, $b_0 = t_1 + t_2$. The two p-wave states are degenerate and the energy is $-a_0$. In the parameter region $-b_0 < a_0 < b_0$ and $b_0 > 0$ (suitable for Cu oxide, see Fig. 4 caption), the s-wave state has the highest energy.[10] The optical experiment measures the dipole active mode at $k=0$. Because of the d symmetry of the Cu hole, both the s- and d-wave modes are optically forbidden. The p-wave modes are optically active, and the charge-transfer gap is given by

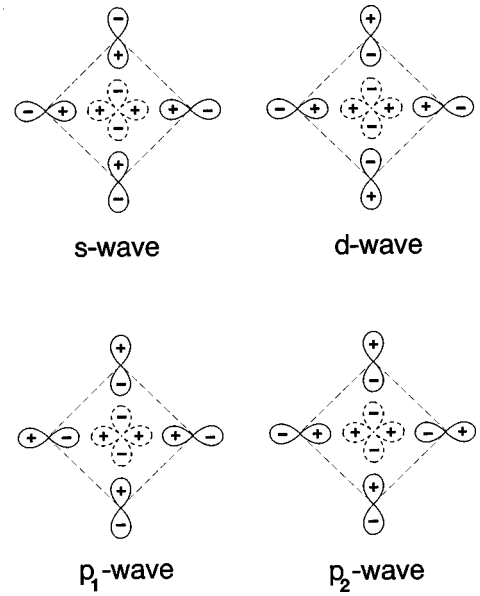

FIG. 3. Symmetries of the four-molecular exciton wave functions, s and d waves in Eq. (7), and the two p waves in Eq. (9) with $k_x = k_y$. The center d wave represents Cu^+, a vacancy at the Cu site. The oxygen $2p_x(2p_y)$ hole wave functions are represented by their orbitals. Only charge degrees of freedom are shown. The implicit spins are the same as in Fig. 1.

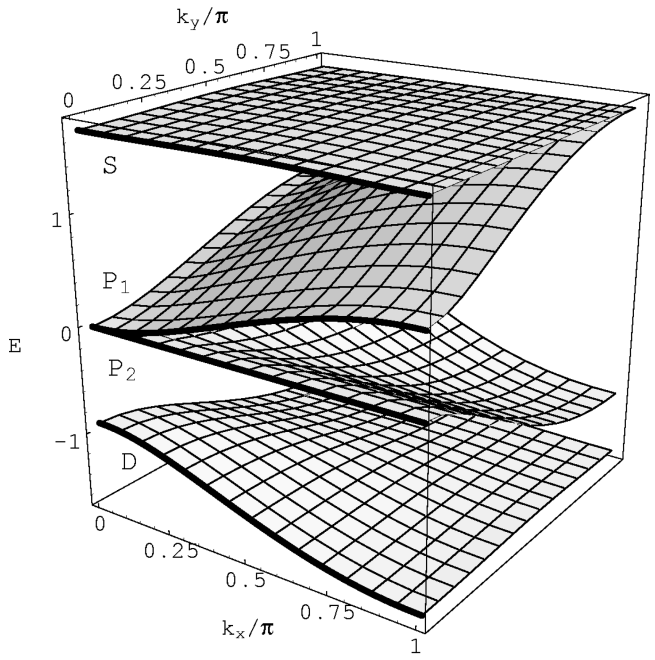

FIG. 4. Calculated exciton energies E (eV) as a function of $\mathbf{k}=(k_x,k_y)$, for the parameters $t_1=0.4$, $t_2=0.126$, $t_3=0.85$, and $t_4=0.65$ eV. The energy is measured relative to the p_1 mode at $\mathbf{k}=0$. The thick solid lines show the dispersions along the [10] direction. The dispersions of the P-wave mode are compared very well with the EELS along the [10] and [11] dispersions. See Ref. 3 for the detailed comparison.

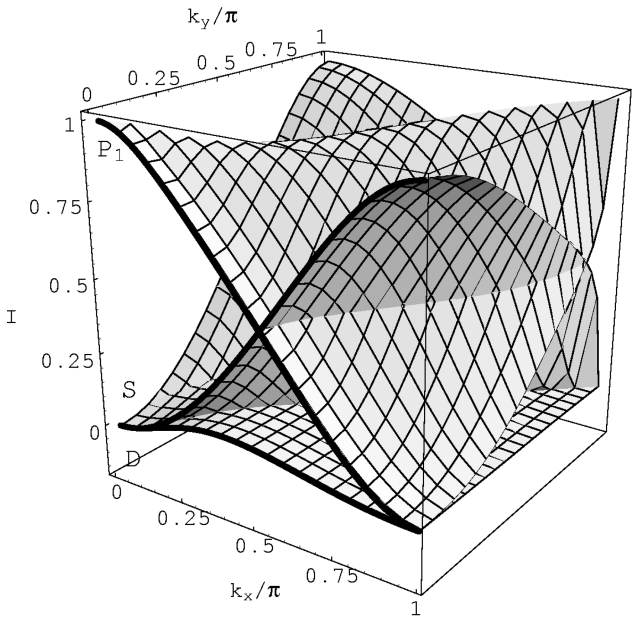

FIG. 5. Calculated intensities I (arb. unit) of the exciton transitions as a function of $\mathbf{k}$, normalized to I_0. The parameters are the same as those in Fig. 4. The thick solid lines show the intensities along the [10] direction. The P_2 mode is not shown because it is dipole inactive and has no contribution to the intensity for all $\mathbf{k}$. The theory is compared well with the EELS along the [10] and [11] directions. The intensities for the S mode at finite $\mathbf{k}$ along [10] were observed in the EELS; see Ref. 3.

$$\Delta=\epsilon_p-E_b-a_0. \tag{8}$$

For finite k along an arbitrary direction $\hat{k}$, the eigenstate of the exciton is a linear combination of the molecular states. We shall denote the four exciton modes by P_1, P_2, S, and D, according to their symmetries p_1, p_2, s, $d_{x^2-y^2}$ in the limit $k\to 0$. For the two p states, we define a dipole active mode $|p_1\rangle$ and a dipole inactive mode $|p_2\rangle$ as

$$|p_1\rangle=(-k_x,-k_x,k_y,k_y)/(\sqrt{2}k),$$
$$|p_2\rangle=(k_y,k_y,k_x,k_x)/(\sqrt{2}k). \tag{9}$$

The exciton dispersions are plotted in Fig. 4. The parameters are chosen[11] to fit the measured EELS.[3] The dispersions are anisotropic. The $E-\mathbf{k}$ relation of the P_1 mode is monotonic, and the energy is peaked at $\mathbf{k}=(\pi,\pi)$. The dispersion width is $2t_3\sim 2t_{pd}^2/\epsilon_p$, which is a large-energy scale, order of the hole-hopping integral in cuprates, but much larger than the dispersion width of the single-hole motion in the AF background, which is $\sim J$.[7] This result is consistent with the EELS.[3] The dispersion along the [10] direction is much flatter, also consistent with the EELS. As we can see from Fig. 4, the lowest energy mode is the D mode. This is in agreement with the weak-coupling method of Littlewood *et al.*[12]

In the EELS, an incident electron is inelastically scattered to create a pair of electron holes with energy and crystal momentum (ω, $\mathbf{k}$). The EELS directly measures Im $[-1/\epsilon(\mathbf{k},\omega)]$, with $\epsilon(\mathbf{k},\omega)$ the dielectric function, hence probes the dispersion and the symmetry of the charge-transfer excitation.[13] For an exciton, the intensity in the imaginary part of $\epsilon(\mathbf{k},\omega)$ around a pole is

$$I=\text{const}\times k^{-2}|\langle\Psi_{ex}|e^{i\mathbf{k}\cdot\mathbf{r}}|GS\rangle|^2, \tag{10}$$

where Ψ_{ex} is the exciton state. For small $\mathbf{k}$, the most dipole active excitations in the EELS can be identified to be the P_1 mode. The dispersion obtained from the EELS (Ref. 3) compares well with the theory. As k increases, the S- and D-mode excitons gradually become EELS, active because of the mixing of the $|p_1\rangle$ molecular state and because of the quadrupole contribution. It is difficult to make a quantitative comparison between the dipole and quadrupole contributions in the S or D mode. However, if the radius of the Cu $3d$ state is much smaller than the lattice constant, the dipole contribution is more important. We expect this to be the case in cuprates. Within the dipole approximation, we have

$$I=I_0|\langle\Psi_{ex}|p_1\rangle|^2, \tag{11}$$

where I_0 is the dipole-active intensity of the P_1 mode at $\mathbf{k}=0$. Note that the total dipole-active intensity of the four modes is conserved to be I_0. In Fig. 5, we show the calculated intensity I of the excitons in Eq. (11) as functions of $\mathbf{k}$. Along the [10] direction, as k increases, the intensity of the S mode increases rapidly, while the intensity of the P_1 mode decreases. The intensity along [11] is quite flat for the P_1 mode and remains to be zero for the S mode. This anisotropy is due to the symmetry of the exciton states. The S-mode eigenstate along [11] contains only s and p_2 states, and both are dipole inactive. Furthermore, the transition matrix from the quadrupole contribution is proportional to

$\langle \Psi_{ex}|e^{i\mathbf{k}\cdot\mathbf{r}}|GS\rangle$, which is $(k_x^2-k_y^2)$ for the s state.[14] Therefore, the intensity for the S mode along [11] vanishes up to the quadrupole order. These features are in excellent agreement with the EELS experiment,[3] where an optical-forbidden transition was observed along the [10] but not along the [11] direction, and the intensity of the optical-active transition along the [10] direction is observed in the experiment to decrease as $\mathbf{k}$ increases.

The D-mode exciton, expected from the theory, is another optical-forbidden state. The current EELS has not revealed this mode, probably due to the limit of the experiment resolution. Further spectroscopy measurements are needed to verify this d-wavelike state. This mode can be active in the phonon-assisted optical process, and should be observable in the luminescence experiment. A recent optical absorption measurement indicates a very weak absorption state at about 0.5 eV in the undoped cuprates.[14] The d-symmetry state is an alternative to the magnon state or crystal-field exciton proposed earlier for this weak absorption where the phonons could be involved.

V. DISCUSSIONS

In this paper we discussed small excitons in the insulating Cu-oxide planes. These are the charge-transfer excitations, which are separated from the lower-energy excitations by an energy order of ϵ_p. The lower-energy excitations are the magnons described by the spin-1/2 Heisenberg model are half-filled. In the doped case, the lower energy charge excitations are given by the hole motion in the AF spin background described by the two-dimensional t-J model.

We have used a local model to describe the excitons in Cu-oxide planes. If we include the individual kinetic energies of the quasiparticle and the quasihole, the excitons should have spatial extensions. The size of the exciton is determined by the balance of the kinetic energies and the Coulomb attraction E_c. This spatial extension will lower the exciton energy. The exciton motion will be more complicated, and will contain an incoherent part disturbing the AF background. The large dispersion width observed in the EELS may be viewed as an experimental indication that the spatial extension of the exciton does not play an important role and the small exciton proposed here may be a good approximation.

We may abstract some physical parameters of the cuprates from the EELS in our theory. The charge-transfer gap given in Eq. (8) may be viewed as a renormalized atomic energy difference between the O and Cu holes. The most reliable parameter from the EELS is the dispersion width along the diagonal direction, which is given, in our theory, by $2t_{pd}^2/\epsilon_p - 2t_{pd}^2/(\epsilon_p+U_{pp})$. This width is about 1.7 eV from the EELS, and is consistent with the parameter estimated from the angular-resolved photoemission experiments, from which the parameter t in the t-J model is estimated to be 0.4 eV.[15] Within the perturbation, $t=t_{pd}^2/(2\epsilon_p)+t_{pd}^2/(U_d-\epsilon_p)-0.5t_{pp}$, where U_d is the on-site Coulomb repulsion at the Cu site. We may consider $t_{pd}^2/\epsilon_p=1.3$ eV, and $U_{pp}=3\epsilon_p$. Then from the EELS, we have $t_{pd}^2/\epsilon_p=1.1$ eV. This is consistent with the estimate of $t=0.4$ eV if we assume reasonably $U_d=5\epsilon_p$ and $t_{pp}=0.65$ eV. Note that the parameters t_1, t_2, and t_4 in Fig. 4 are less sensitive in the fitting to the EELS, and one has to be cautious to use them in a serious estimate for the accurate parameters of the cuprates.

We have so far not considered the electron-hole (e-h) continuum, which starts at energy $\Delta_{e\text{-}h}=\epsilon_p-E_s+E_{kin}$, where $E_{kin}<0$ is the lowest kinetic energy of the independent Cu^+ and the formal Cu^{3+}. For the cuprates, $|E_{kin}|\sim 1-2$ eV. We expect the e-h continuum to start above the $\mathbf{k}=0$ p_1 mode, and the exciton spectra extend into the e-h continuum due to the large spectral dispersion. The states within the continuum region will then be damped, but can exist as resonant states contributing to the EELS. Since the contributions to the EELS from the e-h continuum have much less $\mathbf{k}$ dependence, the excitons become the dominant source of the $\mathbf{k}$-dependent spectra in the EELS.

Our model applies to the insulating phase. In the metallic phase the Coulomb attraction between the quasihole and the quasiparticle is substantially reduced due to the metallic screening, and is too weak to bind a pair.

In conclusion, we have studied a local exciton model for the insulating Cu oxides. The exciton moves through the lattice almost freely in the AF spin background. The model is in excellent agreement with the recent EELS in the insulating $Sr_2CuO_2Cl_2$.

ACKNOWLEDGMENTS

We wish to thank Y. Y. Wang and M. V. Klein for numerous discussions on both experimental and theoretical aspects related to the present work. We would also like to thank T. M. Rice and C. M. Varma for useful discussions. The work was supported in part by DOE Grant No. DE/FG 03-98ER45687.

[1] P. W. Anderson, Science **235**, 1196 (1987).

[2] F. C. Zhang and T. M. Rice, Phys. Rev. B **37**, 3759 (1988).

[3] Y. Y. Wang, F. C. Zhang, V. P. Dravid, K. K. Ng, M. V. Klein, S. E. Schnatterly, and L. L. Miller, Phys. Rev. Lett. **77**, 1809 (1996); **75**, 2546 (1995).

[4] B. O. Wells, Z. X. Shen, A. Matsuura, D. M. King, M. Kastner, M. Greven, and R. J. Birgeneau, Phys. Rev. Lett. **74**, 964 (1995).

[5] D. C. Mattis and J. P. Gallinar, Phys. Rev. Lett. **53**, 1391 (1984).

[6] S. Uchida, T. Ido, H. Takagi, T. Arima, Y. Tokura, and S. Tajima, Phys. Rev. B **43**, 7942 (1991).

[7] See, for example, Z. Liu and E. Manousakis, Phys. Rev. B **45**, 2425 (1992); E. Dagotto, R. Joynt, A. Moreo, S. Bacci, and E. Gagliano, *ibid.* **41**, 9049 (1990); D. Poiblanc, T. Ziman, H. J. Schulz, and E. Dagotto, *ibid.* **47**, 14 267 (1993); G. Martinez and P. Horsch, *ibid.* **44**, 317 (1991); P. W. Leung and R. J. Gooding, *ibid.* **52**, 15 711 (1995).

[8] Some exciton hopping processes, such as $\tau_x(\mathbf{R})\rightarrow\tau_x(\mathbf{R}+\hat{y})$, may

disturb the AF spin background. But these integrals are small, at least fourth order in t_{pp} or t_{pd}, and their contribution to the exciton dispersion is insignificant.

[9] M. J. Rice and Y. R. Wang, Phys. Rev. B **36**, 8794 (1987).

[10] This is consistent with the local molecular picture. The intramolecular energies of the exciton states are $2t_1$ for the s wave, $-2t_1$ for the d wave, and zero for the two p-wave states. This leads to the same conclusion that the S mode has the highest energy provided at $t_1>0$.

[11] There are two nearby peaks in the optical-forbidden transitions observed in the EELS in Ref. 3. Here we assume the lower-energy state to be the S-mode exciton discussed in the text. A smaller t_1 gives a sharper drop in the intensity of the P_1 mode along the [10] direction.

[12] P. B. Littlewood, C. M. Varma, S. Schmitt-Rink, and E. Abrahams, Phys. Rev. B **39**, 12 371 (1989).

[13] S. E. Schnatterly, *Solid State Physics* (Academic Press, New York, 1979), Vol. **34**.

[14] Similar to the discussion for the EELS anisotropy in $BaBiO_3$, see Y. Y. Wang, V. P. Dravid, N. Bulut, M. V. Klein, S. E. Schnatterly, and F. C. Zhang, Phys. Rev. Lett. **75**, 2546 (1995).

[15] S. Haas, A. Moreo and E. Dagotta, Phys. Rev. Lett. **74**, 4281 (1995).